

Characterization of the Molecular Weight Distribution of High-Density Polyethylene by a New Method Using the Turbidity at a Lower Critical Solution Temperature

Alla Barbalata,[†] Takouhi Bohossian, Karel Procházka,[‡] and Geneviève Delmas*

Chemistry Department, Université du Québec à Montréal, C.P. 8888 Suc. A, Montreal, H3C 3P8 Canada. Received June 22, 1987; Revised Manuscript Received March 10, 1988

ABSTRACT: The molecular weight distribution of linear high-density polyethylene (PE) has been measured by a new method using the turbidity at a lower critical solution temperature (LCST). The MW dependence of the LCST (T) is given by $T = T_{\infty} + BM^{-1/2}$ (eq 1), where T_{∞} is the LCST for an infinite MW. The constants T_{∞} and B , characteristic of a given polymer-solvent system, can be obtained from the LCST's of samples with a narrow MW distribution. 2,4-Dimethylpentane has been used as solvent. The technique consists of obtaining a thermogram which is the recording of the maxima (h_i) of the peaks of turbidity provoked in a solution by a succession of temperature increases ΔT_i during phase separation. The elevation of temperature leads to the phase separation of the smaller and smaller MW between T_0 and T_f , the temperature of the initial and final turbidity peaks. Typically, $T_f - T_0$ ranges between 30 and 100 K for samples whose polydispersity M_w/M_n lies between 1.1 and 10. Separation is effected, at each T_i , by allowing the concentrated phase containing the higher MW to fall to the bottom of the tube. The simple relation $m_i = kh_i$ (eq 2) is used with eq 1 for calculating the MW distribution, $w(\log M)$, from the set of h_i , T_i , and T values, the quantity m_i being the concentration of polymer of MW M_i , whose phase separation at T_i creates a turbidity h_i . The thermograms of 10 PE samples of different polydispersity were obtained and their $W(\log M)$'s found in very good agreement with those obtained by the SEC technique. Verification of eq 2 is made by establishing a gravimetric and turbidimetric correlation of the amount of polymer in the concentrated phase between T_0 and T_f . This method, using low-cost equipment and maintenance, can be applied to a variety of solvent-polymer (or copolymer) systems since the LCST is a general phenomena in polymer solutions.

Introduction

Fractionation at a temperature or upper critical solution temperature (UCST) in a solvent or mixture of solvents was used very early on for the characterization of polymers. Integration of fundamental work in thermodynamics and molecular weight distribution (MWD) is presented, for instance, in ref 1a. Parameters affecting the fractionation efficiency (initial concentration, choice of solvent-precipitant)^{1b,c} and use of turbidimetric analysis during fractionation^{1c} have been analyzed extensively. For noncrystalline polymers, or at high temperature for crystalline polymers, cooling the solution or the addition of a non-solvent causes the formation of a concentrated phase in equilibrium with a dilute phase. The higher molecular weights (MW) distributed in both phases are, however, present in greater concentration in the concentrated phase. If the temperature is further reduced, lower and lower MW's enter in the concentrated phase. Quantitative analysis of the amount of polymer present in the concentrated phase leads to the measurement of the MW distribution (MWD) of the polymer.

Raising the temperature of a polymer solution may also produce a liquid-liquid phase separation in the temperature range where a LCST (lower critical solution temperature) occurs. The reduced solubility is due to the increased free volume difference between polymer and solvent near or above the solvent boiling point. Fractionation of polyisobutylene was performed at its LCST in 2-methylbutane.² The advent of steric exclusion chromatography (SEC) (or GPC) as an absolute and universal technique³ discouraged the efforts of using a phase separation at a UCST⁴ or at a LCST⁵ as a method of fractionation and characterization of MW distribution (MWD). However, it would be an advantage particularly for the

characterization of mixtures of polymers to develop a method of MWD determination like the LCST method which would be more sensitive than SEC to the nature of the polymer and the polymer-solvent interaction parameter.

The aim of this paper is to describe the LCST method of characterization and its application to linear polyethylene. The distribution curve and the polydispersity are obtained on polydisperse samples and narrow MWD standards. Results obtained on a variety of PE,^{6a} PIP,^{6b} and PS^{6c} seem to confirm the validity of the assumptions in the present LCST method.

The Lower Critical Solution Temperature. Diminution of the solvent quality when the temperature increases is due to the inescapable difference of expansion between the expanded solvent and the dense polymer. The equation of state theories developed by Prigogine,^{7a} Patterson,^{7b,c} and Flory^{7d,e} predict the occurrence of LCST in nonpolar systems when the difference in volatility of the components is large. Although the trends of the LCST for different polymers in different solvents are well described, the calculated LCST are much lower than the experimental ones. Analysis of the LCST of several polyolefins in nonpolar solvents⁸⁻¹⁰ has shown that polyethylene had LCST values lower than those of the other polyolefins (except polyisobutylene). The difference between the LCST of PE and polypropylene (PP) for instance, which can reach 80 K in a volatile solvent, cannot be accounted for by the difference between the equation of state parameters of PP and PE. This difference in LCST has been explained⁹ in terms of correlations of molecular orientations (CMO) in the concentrated phase of PE. These correlations are not possible in the PP solutions because of the methyl side groups, so that the concentrated phase which is not stabilized by CMO is formed at a higher temperature. LCST values measured for ethylene-propylene (EP) random copolymers show that they lie between the LCST values of the parent homopolymers and can be used as a measure of the copolymer composition.

[†] Present address: Forestry Department, University of New Brunswick, Edmonston, NB Canada.

[‡] Present address: Department of Physical Chemistry, Charles University, Prague, Czechoslovakia.



Figure 1. Thermogram of a solution of polydisperse PE sample (Marlex) in 2,4-dimethylpentane showing the photocell signal at each temperature increment ΔT_i between 130 and 240 °C. The ΔT_i vary from 2 to 9 °C as the MW diminishes. The thermocouple recordings have been deleted from the figure for clarity. The sets of $h_i(T_i)$ are as listed in the Appendix. The turbidity signals for the first three peaks have been marked. For that particular thermogram, the second and third ΔT were effected before the return of the transmitted light to the base line. The h_i are not changed if one waits longer between the peaks.

The LCST is very sensitive to the presence of alkyl groups which occur along the PE chain in the LLDPE. The LCST is raised by even a small comonomer content in the LLDPE due to the diminution of CMO⁹ in the concentrated phase by the alkyl groups.

Measurements of LCST of polyolefins,^{8,9} PS, and other polymers have been made by several groups with a view to testing theoretical predictions. A review of the systems, published prior to 1980, can be found in ref 10. Kleintjens and Koningsveld¹¹ give an accurate prediction of the LCST of PE in *n*-alkanes using a mean-field lattice-gas treatment. The same agreement was also observed with the van der Waals equation of state.^{7e} It is likely that the effect of CMO in lowering the LCST is the reason why LCST have been accurately predicted only for PE systems.

Experimental Section

Solvent. The branched pentane 2,4-dimethylpentane 99% (Aldrich, Milwaukee) was used without purification. The density at 20 °C is 0.6715 g cm⁻³ as compared to literature values of 0.6727. The presence of isomers of heptane of different density can significantly change LCST values.

Polymers. The sources of the polymers analyzed are listed with their respective values of M_w and M_w/M_n in Table I. Apart from the narrow MWD PE standards (Elf-Aquitaine¹² and NBS) the three other samples analyzed, are of two medium and one broader MWD samples: respectively, NBS SRM 1475, a laboratory sample of Dr. Russel (Queen's University, Kingston, Ontario) and a Marlex from Philips. The SEC characterization data are either those given by the supplier or those found in the literature.¹³ The Marlex sample was measured in the Du Pont Research Laboratories in Kingston, Ontario and in the Materials Research Institute (MRIC) in Boucherville, PQ, Canada.

Thermograms. A sealed tube (inner diameter 5 mm, outer diameter 9 mm, length 7–8 cm) containing 0.6 cm³ of the solution in 2,4-dimethylpentane is placed in a small oven whose temperature monitored by means of a temperature programmer TGC85 (Setaram, France) was constant to 0.05 °C. The polymer volume fraction, ϕ_2 , ranges from 0.01 to 0.04. A beam of light is recorded on a photocell after passing through the upper part of the solution. A double-channel recorder is used to register simultaneously the signals from a thermocouple and the photocell. In the present work, the thermogram of a solution is the set of attenuation of light separated by plateaux of high light transmittance developed in time when the temperature is raised by increments as shown in Figure 1. An increase of temperature does not change the transmitted light when it is effected below the first temperature of phase separation, T_0 . Above this temperature, each step of temperature increment leads to turbidity due the scattering of light by the heterogeneous system constituted by the droplets of concentrated phase in the dilute phase. Within

a few minutes at high temperature, or 1 or 2 h at low temperature for the very high molecular weights, the transmitted light is restored to its original value because the droplets have grown and fallen to the bottom of the tube where the concentrated phase gathers. The volatile solvents used preferentially for LCST analysis have a low density at the temperatures at which the LCST's occur, so that the concentrated phase is denser than the dilute phase. The technique uses gravity for separating the different fractions. Each increase of temperature leads to the formation of a new concentrated phase, richer in lower MW's than the fraction formed at the preceding step of temperature. The newly formed concentrated phase ultimately falls to the bottom of the tube, joining what was formed previously. The assumption on which a quantitative measurement of the MWD rests is of a relationship between the maximum of the peak of turbidity h_i produced by a temperature increase ΔT_i and the amount, m_i , of polymer phase separating during this temperature interval in the volume of solution under scrutiny. The end of the thermogram is marked by the temperature, T_t , at which a temperature increment does not lead anymore to a measurable amount of turbidity in the solution. With a rate of temperature increase, ν , varying between 0.8 and 4 K/min, the increase of turbidity is very sharp, the maximum being attained after 1 or 2 min. The increase of temperature is not fast enough for spinodal decomposition to take place because of the low viscosity of the solution at the temperature of phase separation.

A turbidimetric trace of the solution can be obtained also with a constant-temperature ramp. In that case, the thermogram takes the shape of a single peak starting at T_0 . Analysis of mixtures of polymers¹⁴ indicates that if the LCST of the different polymers present are sufficiently far apart, each polymer gives a separate peak at a T_0 value which permits its identification.

The distribution of the initial polymer between the two phases in equilibrium in the tube above T_0 can be measured at any temperature, by weighing the amount of polymer they contain, after evaporation of the solvent. The separation of the phases is made by taking advantage of their different viscosities at low temperature. The bottom of the tube with the concentrated phase is quickly cooled from the temperature of the oven to -80 °C and the tube turned upside down to let the dilute solution flow to the other end of the tube. The glass is then cut to recuperate the two phases separately. This method has been used as a justification of the assumptions as will be described below.

Analytical fractional phase separation and turbidimetric analysis at a UCST or Θ -temperature, commonly known as turbidimetric titration (TT), was reviewed in the 1970s by Urwin⁴ who stressed the inherent difficulties of the method. However, Taylor and Graham reported¹⁵ satisfactory analysis of the polydispersity of PE samples by TT. At an LCST, the TT has gained several advantages over that done at a lower temperature. This is the simplicity of using a temperature increase (rather than a nonsolvent or a temperature decrease) as the agent of phase separation and the effect of the elevated temperatures (situated between T (boiling) and T_c , the liquid-vapor critical temperature of the solvent) in increasing the speed of homogenization of the solution at a molecular scale below T_0 and that of thermodynamical phase equilibrium above T_0 . Since the difference in free volume between polymer and solvent is the main contribution to the χ -parameter at the LCST, the temperature at which phase separation occurs and the MW dependence of the LCST⁸ (see Appendix) can be fairly well predicted. Consequently, one can choose a solvent or a mixture of solvents which optimizes a good dissolution with a low LCST.

Cloud-Point Curves for the Standards. The temperature T_0 of the first turbidity is plotted in Figure 2 against ϕ_2 for the PE standards. For these narrow MW fractions, T_0 does not vary by more than 2–3 K for 0.01 < ϕ_2 < 0.04. The minimum of the cloud point curve of a given MW has been used systematically to define the LCST of a given MW. In Figure 2, the LCST is seen to increase as MW decreases. One has to note here that T_0 reflects only the temperature of phase separation for the highest MW in the sample. As will be seen in Figure 3, most of the polymer phase separates at a temperature higher than T_0 , even for a narrow MWD sample.

Sample Heterogeneity and T_0 . The temperature of the first turbidity has been reached either by making a steady increase

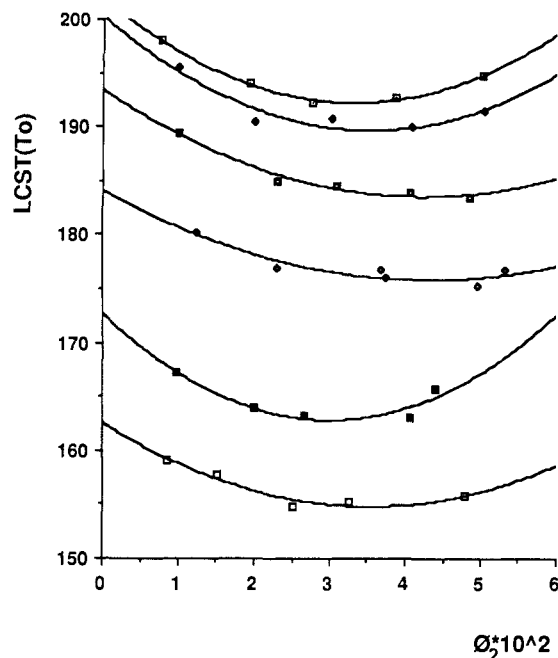


Figure 2. Cloud-point curves, $T_0(\phi_2)$, of solutions of PE standards in 2,4-dimethylpentane. Elf-Aquitaine samples, M in $\text{kg}\cdot\text{mol}^{-1}$: (\square) $M_w = 4.70$, (\diamond) $M_w = 5.80$; (\square) $M_w = 6.70$; (\diamond) $M_w = 8.40$; (\blacksquare) $M_w = 11.60$; (\square) $M_w = 31.30$. The curves for NBS 1475 and Marlex (not shown here) are steeper and have a minimum at 137 and 132 $^{\circ}\text{C}$ respectively.

of temperature or by temperature increment. The cloud-point curves of the samples reported in Figure 2 have been obtained by a constant temperature ramp of 0.8 K/min. The reproducibility in T_0 of the same solution or of another solution of the same concentration is better than 1 K for the narrow MWD samples such as the standards and the Russel sample. On the other hand, for the Marlex (presented in pellets), the reproducibility in T_0 , which is also very good when measured on the same solution, is poor when several solutions are analyzed successively. This is attributed to the small quantity of the polymer needed for the measurement (5–20 mg), which is not sufficient to assure random sampling. If a dozen different tubes of this polydisperse polymer of the same concentration are run through the oven, a medium T_0 value is found more frequently with a few extreme values about 4 deg lower or higher than the medium value. Consequently, when new solutions are made to obtain the whole thermogram, only tubes with the medium value of T_0 are selected for complete analysis. Differences in the amount of high MW in the sample are the cause of the scatter in T_0 . Shear-induced degradation during industrial processes or sample heterogeneity could be spotted rapidly by measuring T_0 rather than the whole thermogram.

No oxidative degradation was detectable by IR after running the solution a few times between T_0 and T_f . Nonoxidative degradation is also unlikely due to the reproducibility of the thermogram and of T_0 in particular, at the second run.

Care must be taken to assure a good homogenization of the solutions, the concentrations of which are higher than those used for characterization by other methods. Aggregates left in the solution tend to lower T_0 as was observed with the medium MW standard NBS 1484.

Results and Discussion

Cumulative Turbidity Curves. In Figure 3, the data given by the thermogram $h_i(T_i)$ are plotted cumulatively versus T_i for the three samples of different MW and polydispersity but analyzed at the same concentration and with about the same temperature programming. The normalized h_i , h_i^* , has been obtained by dividing by the total sum, h_i , between T_0 and T_f . In Figure 3, h_i^* corresponds to the partial sum h_i divided by the same factor. Three characteristic temperatures can be noted on the

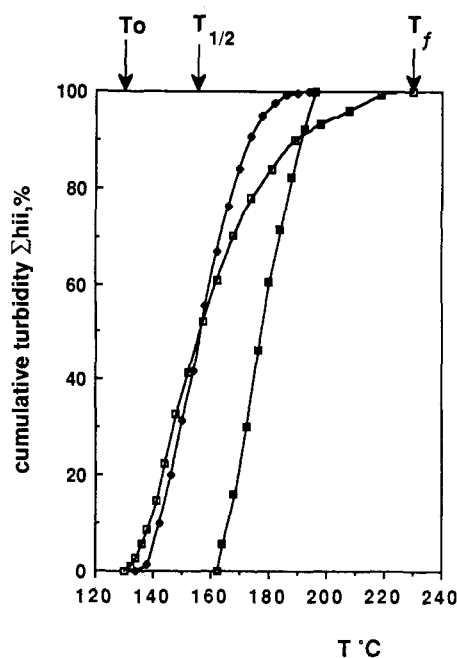


Figure 3. Normalized cumulative turbidity curves Σh_i^* versus T for three samples of different polydispersity, M in $\text{kg}\cdot\text{mol}^{-1}$: (\blacksquare) MS5, $M_w = 32.0$, $M_w/M_n = 1.15$; (\circ) NBS 1475, $M_w = 54.2$, $M_w/M_n = 2.96$, and (\square) Marlex, $M_w = 155.0$, $M_w/M_n = 10$. T_0 and T_f are the temperatures of the initial and final appearance of turbidity and $T_{1/2}$ that at which half the turbidity has been evolved. Note that the $T_f - T_0$ increases with the polydispersity (respectively 20, 56, and 98 K for the three samples).

thermogram: T_0 , the temperature of the start of the first turbidity; $T_{1/2}$, the temperature at which half the turbidity has been obtained; and T_f , the temperature of the end of the thermogram. They are indicated on Figure 3 for Marlex (\square). The values of T_0 increase from Marlex to NBS 1475 (\diamond) and to NBS 1483 (\blacksquare) as the polymer MW decreases.

The interesting result is the value of the temperature interval $T_f - T_0$, that is needed to displace the polymer from the dilute to the concentrated phase when polydispersity changes. The intervals $T_f - T_0$ are 98, 56, and 32 K for the three samples whose polydispersities are respectively 8–10, 2.3, and 1.15. Similar cumulative turbidity curves have been obtained for the other standards and their characteristic temperatures are listed in Table I.

Quantitative Treatment of the Data. In order to translate the cumulative turbidity curves $\Sigma h_i^*(T_i)$ into a MW distribution curve, a calculation is made in the following steps. The temperature scale is transformed into a MW scale by the relation (see Appendix)

$$T_i = T_{\infty} + BM_i^{-1/2} \quad (1)$$

and the turbidity scale into a polymer concentration scale m_i by the simple expression

$$m_i = kh_i \quad (2)$$

The MW distribution function is usually calculated by differentiating the cumulative weight curve by MW. Since no simple analytical expression can reproduce the cumulative turbidity curve and also because there is not much scatter in the data, the distribution curve has been built, point by point, from the individual h_i^* 's. If relation 2 is valid with the same value of k over the range of temperature $T_0 - T_f$, M_w and M_n are found to be

$$M_n = \Sigma(h_i^*/M_i)^{-1} \quad M_w = \Sigma h_i^* M_i \quad (3)$$

and the distribution function $W(\log M)$ can be written as

Table I
Characterization of Linear PE Samples of Different Molecular Weight Distribution by the SEC and LCST Methods

samples	SEC			LCST			$T_{\infty} = 130, B = 5000$			$T_{\infty} = 128, B = 6000$			$T_{\infty} = 128, B = 6000$		
	$T_{\infty} = 130, B = 5000$			$T_{\infty} = 128, B = 6000$			$T_{\infty} = 130, B = 5000$			$T_{\infty} = 128, B = 6000$			$T_{\infty} = 128, B = 6000$		
	$M_w, \text{kg mol}^{-1}$	$M_n, \text{kg mol}^{-1}$	M_w/M_n	$M_w, \text{kg mol}^{-1}$	$M_n, \text{kg mol}^{-1}$	M_w/M_n	$M_w, \text{kg mol}^{-1}$	$M_n, \text{kg mol}^{-1}$	M_w/M_n	$M_w, \text{kg mol}^{-1}$	$M_n, \text{kg mol}^{-1}$	M_w/M_n	$M_w, \text{kg mol}^{-1}$	$M_n, \text{kg mol}^{-1}$	M_w/M_n
Elf-Aquitaine ^a	4.70	<1.10	4.60	4.50	1.03	4.50	4.60	1.03	4.50	4.50	1.03	4.50	4.50	1.03	4.50
MS1 ^b	5.80	<1.10	5.30	5.10	1.02	5.80	5.30	1.02	5.80	5.30	1.02	5.80	5.30	1.02	5.80
MS2 ^b	6.75	<1.10	6.03	5.75	1.05	6.50	6.03	1.05	6.50	6.03	1.05	6.50	6.03	1.05	6.50
PE6750 ^b	11.60	1.15	11.20	9.20	1.15	12.10	10.5	1.14	14.70	12.90	1.13	16.4	14.70	1.13	16.4
MS5 ^b	31.30	1.04	25.30	24.40	1.04	27.10	26.10	1.04	32.20	31.20	1.03	156	160	1.03	156
MS6 ^b	32.00	1.10	27.30	24.90	1.09	29.10	26.60	1.09	34.40	31.80	1.08	154	159.2	1.08	154
1483 ^b	119.60	1.20	114.20	75.75	1.50	116.90	79.30	1.47	124.30	89.40	1.39	138	144	1.39	138
1484 ^b	54.20	2.96	53.60	25.10	2.10	55.60	26.90	2.10	61.20	32.30	1.90	157	157	1.90	157
1475 ^d	155.00	10.00	170.30	15.90	10.65	147.10	17.25	8.50	119.10	21.20	5.60	132	157.6	5.60	132
Marlex ^e	100.00	8.00	797.30	212.70	3.75	693.50	216.80	3.19	525.50	226.60	2.32	133	137	2.32	133
Philips	500.00	~2	797.30	212.70	3.75	693.50	216.80	3.19	525.50	226.60	2.32	133	137	2.32	133
IGM															
Russel ^{b,f}															

^aReference 12. ^bSamples used as standards in Figure 3. ^c T_0 at the concentration used for the thermogram (0.02 < ϕ_2 < 0.04) may be 1–2 K higher for the high MW than the minimum of the cloud-point curve. ^dAs given by the National Bureau of Standards. Other GPC results give a lower value of M_w/M_n , namely, 2.30¹³ and 2.25 (IGM). Good agreement has been found for M_n (18.0 kg mol⁻¹) by using NMR.³³ ^eThe highest values have been found in the Du Pont Research Laboratory (Kingston) and the lowest at IGM (Varennes, Canada). The Wesslau distribution function, with the h_i^* , leads to $M_w = 170.0$ kg mol⁻¹ and $M_w/M_n = 9$. ^fThis sample was made in Dr. K. Russel Laboratory (Kingston). It is nominally a random copolymer of ethylene and butene. However, the methyl content as measured by IR is too small to be detected. The sample is used for the calibration as a high MW, linear, high-density PE.

$$W(\log M) = d \sum h_{ii}^* / d \log M =$$

$$h_i^* / (\log M_i(T_i) - \log M_i(T_i - \Delta T_i)) \quad (4)$$

where ΔT_i is the temperature increment which gives rise to the turbidity h_i^* .

By use of eq 1, eq 3 and 4 can be simplified to

$$M_w = \sum h_i^* M_i = B^2 \Gamma(h_i^* / (T_i - T_{\infty})^2)$$

$$M_n = \sum (h_i^* / M_i)^{-1} = B^2 (\sum h_i^* (T_i - T_{\infty})^{-1})^{-1}$$

$$M_w / M_n = \sum (h_i^* / (T_i - T_{\infty})^2) \sum h_i^* (T_i - T_{\infty})^{-1} \quad (5)$$

and

$$W(\log M_i) = h_i^* (2 \log (1 + \Delta T_i / (T_i - T_{\infty})))^{-1} \quad (6)$$

Since the quantity $W(\log M_i)$ corresponds to the amount of polymer which has entered the concentrated phase, between $T_i - \Delta T_i$ and T_i , it will be associated in the plots of $W(\log M)$ with a value of M intermediate between M_i and $M_i(T_i - \Delta T_i)$, namely $(M_i(T_i)M_i(T_i - \Delta T_i))^{1/2}$.

It is interesting to note that the distribution function and the polydispersity do not depend explicitly on the constant B in eq 1.

If T_0 is explicated in eq 4 and 5, one finds

$$M_w = (B / (T_0 - T_{\infty}))^2 \sum h_i^* / (1 + \Delta T_i / (T_0 - T_{\infty}))^2 \quad (7)$$

$$M_n = (B / (T_0 - T_{\infty}))^2 / (\sum h_i^* (1 + \Delta T_i / (T_0 - T_{\infty}))^2) \quad (8)$$

$$M_w / M_n =$$

$$\sum \frac{h_i^*}{(1 + \Delta T_i / (T_0 - T_{\infty}))^2} \sum (h_i^* (1 + \Delta T_i / (T_0 - T_{\infty}))^2) \quad (9)$$

$$W(\log M_i) = h_i^* \left(2 \log \left(1 + \frac{\Delta T_i}{T_0 - T_{\infty} + \sum_{i=1} \Delta T_i} \right) \right)^{-1} \quad (10)$$

If a constant step, ΔT , is used in the thermogram, one should replace ΔT_i by ΔT and $\sum_{i=1} \Delta T_i$ by $i \Delta T$. In the same equation, T_{∞} is the LCST for the infinite MW and T_0 the temperature of the first turbidity for the sample under study.

Calibration Curve with the Standards. Since the standards phase-separate over a considerable temperature interval, their "average LCST" has to be defined. $T_{1/2}$ is a convenient definition which corresponds either to M_w or M_n for the monodisperse sample and to an average in molecular weight intermediate between M_w and M_n for the polydisperse samples. The $T_{1/2}$ values are plotted along with the T_0 versus $M^{-1/2}$ in Figure 4. Both series of data follow the $M^{-1/2}$ law in agreement with eq 1. A given increment of T gives the same increment in units of $M^{-1/2}$ across the whole MW range. This means that a constant T will correspond to a larger MW interval at the lower temperature or higher MW region. Vice versa, if samples of the same polydispersity are compared, the interval of temperature on which the whole polymer will phase separate, i.e., $T_f - T_0$ (or part of this interval, $T_{1/2} - T_0$), will decrease as the MW increases. This can be seen in Figure 3 where the T_0 and $T_{1/2}$ lines come close together at low temperature and also from the data in the last columns of Table I. One would have expected the two curves to extrapolate to the same T value. The difference of three degrees observed between the two limiting values could probably be diminished by using narrower MWD high MW standards. Since narrow MWD samples with a high MW are difficult to find, a laboratory sample of linear PE made in Dr. K. Russel laboratory was used to complete the curve. The value of $T_{1/2} - T_0$ for that sample is one of the smallest

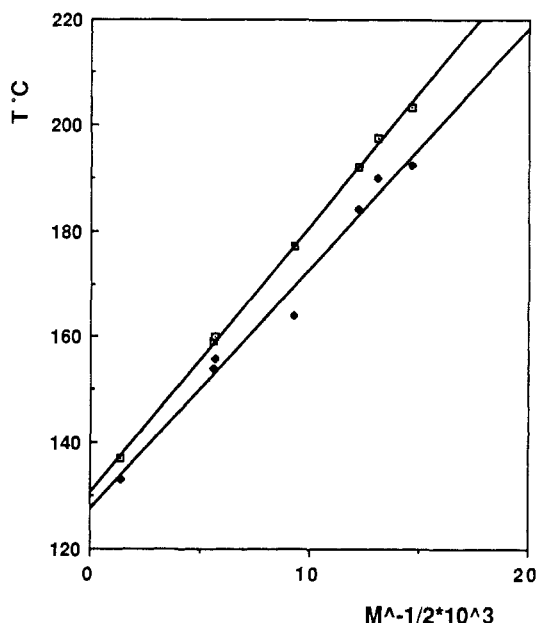


Figure 4. Calibration curve in 2,4-dimethylpentane with the standards T_0 (●) and $T_{1/2}$ (◻) are plotted against $M_w^{-1/2}$ for the samples described in Figure 2 and for NBS 1484 and the Russel sample. The T and B values are respectively 127.5 °C and 4530 from T_0 and 130.6 °C and 5000 from $T_{1/2}$.

in the series, but its polydispersity is still found to be around 3 because of the high MW. Results of calculations are shown in Table I using three T_∞ values (and the corresponding B) that are intermediate between the two extrapolated T_∞ values. Calculations of $W(\log M)$ were made with the rounded value (130 °C) for T_∞ nearer to the extrapolation of the $T_{1/2}$ line. Polydisperse samples would stand out if plotted in Figure 4: when the Marlex data, for instance, are placed on the graph with M_w as the abscissa, T_0 will not be very different from that of the standard having the same M_w , but the $T_{1/2}$ point will be 17 K higher than the corresponding point on the calibration curve.

Table I gives the characteristics of the samples as obtained from the thermogram data and the calibration curves of Figure 4. The $W(\log M)$ are reported in Figure 5 for three samples Marlex (■), NBS 1475 (◻), and Atochimie MS5 (◆). It is interesting to see that there is very little scatter of the points although no smoothing of the h_{ii}^* curve has been applied. Since no correlation has been made, the $h_i^*(T_i)$ values and T_∞ are the only data needed to reproduce the $W(\log M)$ curve. The B parameter just situates the curve on the $\log M$ axis but does not alter the curve shape.

In Table I, one can note that the polydispersity and M_w of the low MW standards are well reproduced from the h_i^* and eq 7–10 with the same T value (129.5 or 130 °C). The differences between the nominal and calculated characteristics are within a few percent. Sample 1483, on the other hand, would be better calculated with a slightly lower T value (=128.5 °C).

For the polydisperse sample, NBS 1475, the same parameters give MWD characteristics in agreement with the SEC data. This is true also for the Marlex since $T_\infty = 129.5$ °C lead to a M_w differing by 5% of the SEC value obtained by Du Pont. A lower value of T_∞ (=128 °C) would give the data obtained on another SEC apparatus (IGM). The characteristics of the Russel sample have been found by the LCST method to be in agreement with the expected values. Those of the 1484 sample do not seem to be those reported but are similar to those found for the Russel

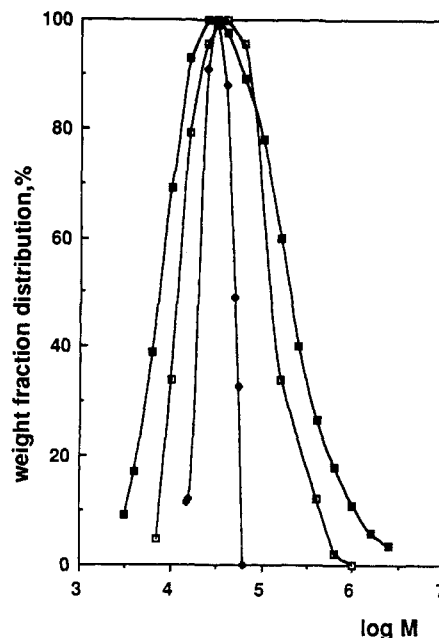


Figure 5. Molecular weight distribution function versus $\log M$ as obtained from eq 5 for the narrow (●), medium (◻), and large (■) MW distribution samples whose cumulative turbidity curves are given in Figure 3.

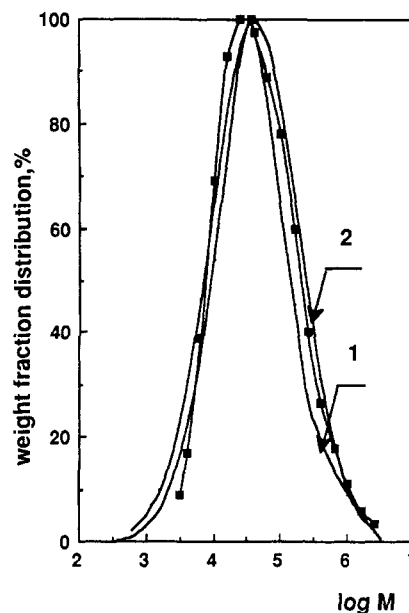


Figure 6. Comparison of the distribution curves for Marlex. The points are calculated from h_i^* and eq 5. Curve 1 is obtained from the h_i^* and the Wesslau distribution function as described in the Appendix (eq 16). Curve 2 is the SEC distribution.

sample (with a slightly wider MWD). In conclusion, Table I results, drawn from a variety of linear PE samples, justify the assumptions underlying eq 1 and 2. Direct justification will be given below.

Comparison of the LCST and SEC Distribution. In Figure 6, three curves of $W(\log M)$ have been drawn for the Marlex sample. The LCST distribution is represented by two curves calculated directly point by point as in Figure 5 and curve 1 from the Wesslau distribution using the experimental h_i^* (see Appendix for the Wesslau expression). The SEC distribution is curve 2. The comparison between the two methods is excellent. The limit of the measurements, at $\log M = 3.5$, is explained below.

Conditions of the Measurements. Effect of the Rate of Heating. It was found from the thermograms of four

standards, made at different rates of temperature increase, ν , that the same $T_{1/2}$ are obtained for $0.8 < \nu < 4$ K/min. Also, $T_{1/2}$ is unchanged when the temperature rise is effected by equal steps of ΔT K for $1 < \Delta T < 4$ K. On the contrary, very rapid increases of temperature ($\nu = 15$ K/min) have the effect of displacing the calibration curve 10 K higher. Several effects may cause this phenomenon but it is possible that thermodynamical equilibrium of the MW's between the newly formed phase and the dilute solution may not be reached in the time needed to develop the turbidity peak. There is no advantage in increasing ν , since the rate-determining factor, for completion of the thermogram, is the time of sedimentation of the concentrated phase and not the time necessary for raising the temperature.

Choice of the Temperature Increments. The first thermograms were made with uniform temperature increments of 2 K which were later increased to 4 K in order to study the parameters influencing the turbidity. With this temperature programming, the h_i 's have unequal intensity over the thermogram, because of the MW distribution but also because of the form of eq 1 as discussed above. To be in the best conditions for eq 2 to apply, the steps of temperature should correspond to those generating peaks of about the same turbidity or the same amount of polymer phase separating. Equal intervals of $\log M_i$, on the other hand, equivalent to equal values of $\Delta T_i/(T_i - T_\infty)$, lead to a $\Delta T = 0.5$ K at 130 °C and 8 K at 190 °C. A succession of intervals of 1, 2, 3, 4, 5, and 8 K has proved to be a good optimization of the results for a polydisperse polymer. For a low MW standard, a few steps at $\Delta T = 2$ K followed by a series at $\Delta T = 4$ K is reasonable. On the other hand, a few steps of 1 K should be done when high MW is expected. The thermograms which have been made with a uniform temperature interval of 2 K give about the same characteristic for M_w and M_n as those with a variable ΔT , but there is more scatter in the low MW side of the distribution curve due to the small magnitude of h_i^* compared to that of $(2 \log(1 + (\Delta T_i/(T_i - T_\infty))))^{-1}$. This term may take the same value at low and high temperature at the condition that ΔT_i is adjusted. For instance, the log expression above is equal to 4.25 for $\Delta T = 0.5$ at 130 °C and $\Delta T = 8$ K at 190 °C, but it can be larger when ΔT is small at high temperature.

Expansion of the Solvent and Lower Limit on MW Characterization in 2,4-Dimethylpentane. The change of molar volume and of pressure in 2,4-dimethylpentane between 130 °C and its critical temperature, T_c (=247 °C), can be calculated from data¹⁶ on normal heptane whose T_c is 267 °C. At 230 °C, the pure solvent has a vapor pressure of 21 atm and its molar volume has increased by a factor of 1.45 from its value at 130 °C. However, direct measurement of the polymer solution volume under pressure made by following the position of the liquid vapor meniscus revealed that the volume increase is only 11% over the same temperature interval. The h_i between 130 and 230 °C should be compared after a volume correction equal to the ratio of the solution volumes at T_i and T_0 , since the real volume fraction decreases as the solvent expands. However, the results given in Table I or Figures 4 and 5 do not include this correction because the effect is not too large and also because it was thought that uncorrected data are valuable in following the arithmetics between h_i^* and M_w and M_n and $W(\log M)$.

Between 130 and 230 °C, the decrease of density of the solution is not sufficient to change the light transmitted so that the base line is constant to within a few percent. However, above 230 °C, the transmitted light diminishes

rapidly to extrapolate to a null value at T_c . The turbidity peaks due to the polymer phase separating above 230 °C are still distinct when a temperature increment is made and could be added in the cumulative turbidity. By using the equation of state parameters of the solvent and/or the solution, reasonably accurate volume corrections could be made and were important at temperatures approaching T_c . However, for the same reasons as mentioned above, only peaks of turbidity occurring below 230 °C were counted, without correction, in the thermograms. The small amount of polymer phase separating above 230 °C, i.e., whose MW is lower than 2500 ($\log M = 3.4$) (eq 1), is unlikely to be important in Marlex if judged by the low MW end of the distribution curves in Figures 5 and 6. If the detection of small amounts of very low MW is important for correlating structure-rheological properties for instance, a more volatile solvent or a mixture of solvents should be used to reduce the value of the LCST/ T_c ratio and react, without corrections, smaller MW molecules.

Polymer Left in the Dilute Phase. Above 230 °C, the dilute phase contains a quantity of polymer, which, for Marlex ($\phi_2 = 0.04$), corresponds to about 4% of the initial polymer (average of six determinations). By using the technique described above, the amount found in several solutions made in larger tubes was collected and a thermogram of the dilute phase fraction was made at the usual concentration. The thermogram shows a distribution of medium and low MW centered around $\log M = 4$. This fraction should be added, with the appropriate weight, to the original thermogram to obtain the total distribution. As no systematic study was made of the effect of the initial MW on the amount and distribution of the polymer left in the dilute phase, results are given without that correction. Since extraction and characterization of the polymer left in the dilute phase cannot be made in routine measurements, a correction in T_∞ value could be added to take this effect into account. The values of M_w and M_n , calculated by the Wesslau distribution from the present data ($M_w = 122\,600$, $M_n = 13\,000$ for Marlex, with $T_\infty = 129.5$) are lower than those obtained from the point by point method. This is due mostly to the large tail of the distribution given by the Wesslau formula and in part too to the small MW left in the dilute phase above 230 °C.

Justification of the Assumptions. Theories of phase relationships and analysis of fractions indicate that polymer molecules phase separating at T_i do not have a narrow MW distribution around M_i . It is implicit in the present method that eq 1, applied to the fractions, relates T_i to an average MW, M_i , of the polymer chains entering the concentrated phase at the temperature T_i .

Although the satisfying results obtained for $W(\log M)$ and M_w/M_n for Marlex and NBS 1475 constitute an indirect support of the assumptions, some direct tests concerning the validity of eq 1 and 2 have been done and are described below. Since the subject of the validity of eq 2 may be more controversial than that of eq 1, the former will be discussed more thoroughly first.

A. Relation between Attenuation of Turbidity h_i and Amount of Polymer Displaced in the Concentrated Phase m_i (Eq 2). Measurements have been made in this laboratory to study the scattered light at 90° to the incident beam instead of the transmitted light by using a ramp instead of a step by step increase of temperature. The fact that the thermograms obtained in the two ways were mirror images of each other was a confirmation of the value of using the attenuation of transmitted light as a measure of scattered light. The intensity of light scattered by a heterogeneous system such as that formed in a solu-

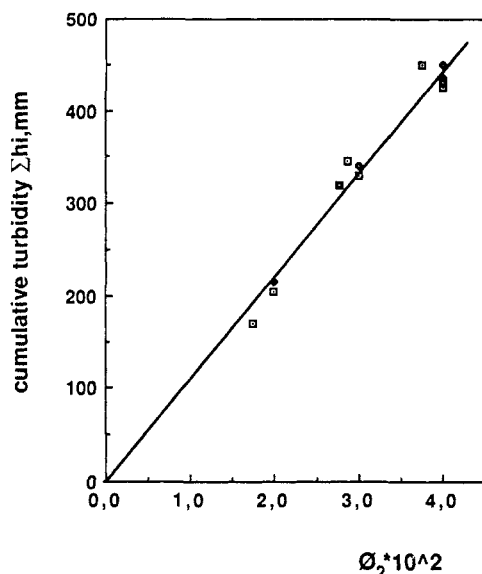


Figure 7. Cumulative turbidity between T_0 and T_i for 11 samples of PE of different MW versus the polymer volume fraction, ϕ_2 .

tion at the onset of phase separation depends on many parameters.⁴ These are the optical terms related to the difference in refractive indices of the dilute and concentrated phases, the number of scattering particles per unit volume, and their size compared to the light wave length. In the actual measurement, two of these three factors may change during the growth, agglomeration, and descent of the droplets down the tube. Beattie and Jung,¹⁷ who measured the light scattered by a dilute solution during phase separation at a UCST, found that the amount of polymer phase separating was indeed proportional to the maximum of light scattered under certain restrictions. Although the present conditions are different from those prevalent in the turbidimetric titration, it is reasonable to assume the linear relationships holds at the LCST also, either for the scattered light or the absorption of light, when the maximum of turbidity caused by a small temperature interval is used in the correlation. The assumption of the constancy of k over the range of temperature of the fractionation seems quite an oversimplification since one would expect the term coming from the difference of refractive indices between the two phases to increase with temperature due to the larger expansion coefficient of the dilute phase.

In order to check the validity of eq 2, the following measurements have been done.

Cumulative turbidity curves have been obtained for solutions of different ϕ_2 , in the range $0.018 < \phi_2 < 0.04$. The cumulative turbidities, reported in Figure 7 for 11 different solutions of different MW, are found to be proportional to ϕ_2 . Another test consists of the comparison of the normalized cumulative curves for several concentrations of the same MW. It has been found that the normalized h_i^* (T_i) curves for the different concentrations overlap over the T_0 – T_i range. Care is taken to have a well-dissolved solution when the MW is high. A simple relationship between m_i and turbidity had not been found as a general case⁴ in the TT at a UCST where addition of a nonsolvent is used to induce turbidity. At a LCST, however, the rapidity of the formation of the concentrated phase, reflected by the short time (1–2 min) necessary to reach the maximum of intensity, may allow the separation of the different contributions to the resulting turbidity. The time necessary to reach the maximum turbidity has been observed not to be concentration dependent in the range of measurements. It is likely that aggregation and

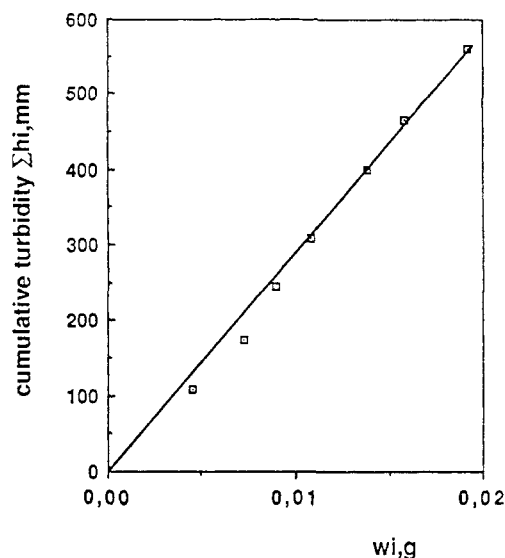


Figure 8. Correlation between the cumulative turbidity obtained from h_i^* between T_0 and T_i and the amount, w_i in milligrams, of polymer in the concentrated phase at T_i . The different points correspond to the different temperatures at which the thermogram has been interrupted and the concentrated phase analyzed (see text). Marlex sample with $\phi_2 = 0.05$.

sedimentation occur only after the maximum of turbidity and do not influence its value.

Correlation of Turbidimetric and Gravimetric Analysis. The constancy of k between T_0 and T_i has been verified as described below. Several solutions at the same concentration were successively heated until a temperature, T_i , different for each tube, and the respective cumulative turbidities, Σh_i , were obtained. The polymer in the concentrated phase was then separated and its weight (w_i) determined gravimetrically for each solution. In Figure 8, the values of w_i are plotted versus the cumulative turbidity for Marlex. Seven points have been obtained over the interval of phase separation. The same measurements have been done for NBS 1483 which phase separates over a smaller temperature interval. The good linear relationship between w_i and h_i^* for Marlex and NBS 1483 (not shown here) is a validation of eq 2 in the range of concentration used in these measurements. The reproducibility of these data is about 5%.

This result is rather surprising if one considers all the factors which may change in the temperature range over which a polydisperse polymer is analyzed. However, in these nonpolar systems, and probably also in polar systems at the usual temperatures of the LCST, the change of physical parameters in the solution (viscosity, refractive index, composition of the phases in equilibrium, interfacial tension between the phases) are all related to the solvent expansion or to the temperature. It is possible that the absence of measurable variation in k over a large temperature interval is due to some canceling of factors. One should note here that the support of eq 2 by the data in Figures 7 and 8 is independent of the value of the parameters T_∞ and B .

Since Figure 8 has established the validity of using h_i as a measurement of the amount of polymer displaced in the concentrated phase, the shape of the cumulative curve becomes an indication of the quality of the dissolution at a molecular level of the polymer below or above T_0 . A solution whose dissolution is inadequate due to too high a concentration or insufficient dissolution time has been found to have less peaks, a value of T_i lower than found at higher dilution, and a steeper cumulative curve. This result is taken as meaning that the smaller MW species

present in the sample have undergone phase separation at low temperature along with the higher MW species and are consequently no longer available for turbidity peaks at high temperature. The fact that further dilution does not change h_i^* is not a proof that the solution is molecularly dispersed but indicates that if association is present, it does not change any more with dilution.

B. Relation between LCST and Molecular Weight (Eq 1). From free volume theories which predict a χ -parameter increasing with temperature and by using the Flory-Huggins combinatorial entropy, eq 1 can be predicted as a first approximation for nonpolar systems (see Appendix). The relation (supported also by Figure 4) has been verified on fractions and particularly on polystyrene standards¹⁸ by using only T_0 to characterize the cloud-point curves (CPC) and not the whole thermogram. In the literature, T^{-1} rather than T has been related to $M^{-1/2}$, in analogy to the relationship used at the UCST, with satisfactory results because the interval of temperature was not sufficient to test the difference between the T and T^{-1} relations.

Effect of Polydispersity on T_0 . In the present calculations of M_w and M_n , eq 1 is assumed to be true for a given φ_2 , whatever the concentrations, φ_i , and the MW and MWD of the surrounding molecules are. The validity of this assumption is supported by the following results concerning T_0 : When two narrow MW fractions ($M_1, T_{0,1}$) and ($M_2, T_{0,2}$) are mixed ($0.01 < \varphi_2 < 0.03$) the temperature of the first turbidity of the mixture has been found repeatedly to be $T_{0,1}$. The insensitivity of T_0 to the average M_w or M_n is indicated also by the fact that the minima of the cloud-point curves of an unfractionated polymer and of its first fraction are the same. The same result was found at the UCST of mixtures of PS fractions:¹⁹ when φ_2 is < 0.05 the cloud-point curve (CPC) of the mixture does not vary by more than 1 K of the CPC of the highest MW fraction. Fractions of LLDPE⁶ have been used to verify also the relation on a series by comparing the highest MW's they contain from their T_0 and eq 1 and from the first signal on the GPC curves. On the other hand, the cloud-point curves of the original polymer and of a fraction do not overlap at higher concentrations. Probably, eq 1 is the most valid in the concentration range of the minimum of the cloud-point curve. The small effect of sample polydispersity on the maximum precipitation temperature at a UCST has been predicted by Shultz^{20a} using a two-parameter distribution function and equations for the chemical potential derived by Tompa.

While the thermogram is developed, differentiation of the concentrations between the phases occurs gradually between the two phases such as $\varphi_2(\text{dilute}) < \varphi_2(\text{initial}) < \varphi_2(\text{concentrated})$. The constants in eq 1 are kept unchanged when the dilution of the dilute phase increases. It is likely that the presence of the concentrated phase in equilibrium with the dilute phase restricts the variation of the chemical potential which otherwise would occur upon dilution. Rayner²⁰ has found that at a UCST, the temperature of phase separation of a lower MW fraction is a function of the concentration of the higher MW species already in the concentrated phase. The conditions of the measurements at the UCST were different from those prevalent here, since a continuous precipitation was used on one hand and also because the interval of temperature needed for the complete phase separation of a narrow MWD sample was only a few degrees at the UCST compared to 20–30 K in the present PE-2,4-dimethylpentane systems. However, the main reason for the high sensitivity of the phase-separation temperatures to the polymer

concentration comes, in the TT work, from the high dilution used (10^{-5} g cm⁻³ or less), as can be expected from the shape of the cloud-point curves at high dilution (Figure 2).

It has been reported in the literature that the presence of low MW polymer increases the solubility of the high MW species. This must be qualitatively even truer at a LCST than at a UCST since the free volume contribution to the χ -parameter will decrease if the average expansion coefficient of the polymer is increased by the presence of low MW species. If the solubility is defined by the value of T_0 , addition of low MW species does not increase solubility. On the other hand, $T_{1/2}$ is raised by this addition (as already mentioned, cf. Table I), in agreement with an increased solubility. This may only mean that solubility is related to an average MW whose value is obviously changed by the addition of low MW species.

Comparison with Other Methods. Modification and additions have been applied over the years to the widely used SEC elution method to shorten the time needed for the measurement or to widen its separating capacities. For instance, in-line MW characterization of the fractions by viscosity measurements,²¹ laser light scattering (LALLS),^{22,23} and turbidimetry²⁴ eliminates the usual calibration with standards and provides an absolute method for copolymers. A new method, the thermal field flow fractionation, introduces the thermal diffusion coefficient of the polymer as a parameter acting on the separation. By this technique,²⁵ mixtures of two samples, unresolved by SEC, can be differentiated. Another elution method is phase distribution chromatography,²⁶ which is based on the interaction of the injected dilute solution of the polymer with a noncross-linked high polymer gel of the same kind. The interaction, which takes place below the θ -temperature of the system, assures a very efficient fractionation. For copolymers, the characterization is dictated by the nature of the sequences. For the LLDPE for instance, fractionated dissolution (temperature rising elution fractionation) takes advantage of the variation of the dissolution temperature of the copolymer with the comonomer content.²⁷ It reveals a heterogeneity in composition of some LLDPE not perceived by SEC. For more complex polymers or copolymers, such as SAN, high performance precipitation liquid chromatography has been used with excellent separating power.²⁸ Band sedimentation chromatography, based on separating particles through their sedimentation velocity, coupled with LALLS detection is particularly suited to high MW polymer characterization.²⁹ Classical light scattering measurements and Rayleigh line width spectroscopy have been used recently to obtain MWD of PE.³⁰ The pulse-induced critical scattering (PICS)³¹ has been developed to explore phase relationships in blends, to assist in refining statistical thermodynamics models, and also to characterize polymer samples. It has in common with the LCST method the measurement of scattered light by a solution at a critical temperature (UCST). There are important differences with the LCST method in the technique and in the theory: Macroscopic phase separation which is desired in the LCST method is prevented in PICS by keeping the solution above the spinodal curve. Also, in PICS only the highest temperature at which light is scattered by the solution is measured for a large range of concentrations and the technique allows the determination of the spinodal. The equivalent (or almost the equivalent since in the PICS method a spinodal curve instead of a CPC is measured) would be to extract, in our method, only from $T_0(\varphi_2)$ (Figure 2) the information about MWD. This is

possible since the chemical potential of the solvent and its derivatives are functions of the MWD and particularly of its higher moments. Since the MWD is obtained through fitting experimental and computed spinoidal curves, good theoretical models adapted to the systems to be studied and theoretical ability are needed to make full use of the PICS method.

From the above description, one realizes that presently existing methods of MWD are the privilege of large laboratories because of their cost and sophistication. The advantages of the present method are its simplicity and flexibility brought about by the choice of solvent. In the nonpolar systems studied here, the simplifying assumptions have been verified. Standards are not essential for the calibration as detailed in the Appendix. Adaptation to copolymers or complex systems such as LLDPE is possible.^{6a}

The aim of this first paper on the LCST method was to give a detailed but not final analysis of its possibilities and limits. As can be judged by the differences noted in Table I between the GPC and LCST techniques, there is scope for improvement either in the acquisition of the turbidity peaks or their treatment and the implementation of the various corrections mentioned above. Calculations made by using the simple van der Waals model, instead of eq 1, to relate T_i to M_i lead to a smaller deviation between nominal and calculated values for M_w and M_n for the low and medium molecular weight samples. This more accurate treatment of the data, which corresponds to using a constant B which diminishes when M decreases, will be presented in a later work dealing with linear low-density PE.

Acknowledgment. We thank Dr. R. St. J. Manley (Pulp and Paper Research Institute, Montreal) for some PE standards, Dr. L. A. Utracki (IGM, Boucherville, PQ) for PE standards and SEC characterization, Dr. E. Keluski (Du Pont Research Center, Kingston, Ontario) for SEC measurements, and Dr. K. Russel (Queen's University, Kingston, Ontario) for a PE standard. The research was made through a NSERC grant given for collaboration between University and Industry (program PRAI), collaboration initiated by Dr. D. G. Robinson at Du Pont.

Appendix

The Constant B . The equation of state theories of liquids permit the calculation of thermodynamic functions such as the enthalpy, entropy, and configurational heat capacity (C_p) of the liquid from the $p = f(v, T)$ equation. The application of these theories to dilute polymer solutions gives an expression for the chemical potential of the solvent in solution in terms of the property of the pure liquid and of parameters expressing the difference between polymer and solvent. In nonpolar system, chemical differences can be neglected so that the χ interaction parameter is given by the simple expression⁸

$$\chi = (C_p/2R)\tau^2 \quad (11)$$

τ^2 is temperature independent and can be calculated from the difference in volatility between solvent and polymer. In the present system $\tau^2 = 0.11$ in 2,4-dimethylpentane while it is 0.09 in the less-volatile normal heptane. C_p increases with temperature at a faster rate when the temperature approaches T_c (C_p goes to infinity at T_c). Using free volume theories or equivalent models, the pressure dependence of the LCST for PE n -alkanes systems and others,^{11,32} has been correctly calculated. At the LCST, as at the UCST, the critical value of χ in the Flory-Huggins theory is given by

$$\chi_c = 0.5 + r^{-1/2} = 0.5 + (\text{const})M^{-1/2} \quad (12)$$

where r is the number of segments in the macromolecules, defined by the ratio of the polymer and solvent molar volumes. In heptane, the constant in eq 12 is about 10.

From eq 11 and 12, one finds that the LCST occurs at a value of C_p which depends on the MW of the polymer.

$$C_p(T_i) = (2R/\tau^2)(0.5 + (\text{const})M^{-1/2}) = 2C_p(T)(0.5 + (\text{const})M^{-1/2}) \quad (13)$$

Around T_i , $C_p(T_i)$ can be developed as

$$C_p(T_i) = C_p(T_\infty) + (\partial C_p/\partial T_i)(T_i - T_\infty) \quad (14)$$

which leads to

$$T_i = T_\infty + 2C_p(T_i)/(\partial C_p/\partial T_i)(\text{const})M_i^{-1/2} \quad (15)$$

From eq 11 and 15, the effect of solvent parameters on the value of the LCST and on the MW dependence at the LCST can be analyzed. In a volatile solvent, τ^2 is large so that the critical value of χ can be reached at a lower value of C_p or of T . By the same argument, one can predict the variation of B with the solvent volatility: When the LCST occurs at a low temperature, far from the critical temperature of the solvent, $\partial C_p/\partial T$ is small, so that B is large. On the contrary, in a less volatile solvent, B will be smaller, because the LCST is reached at a value of T near T_c at which the denominator in the second term of eq 15 will be large since C_p varies fast then with T . The characterization in a volatile solvent, if it is a good enough to assure an adequate dissolution, gives more resolution for the MW distribution.

Using literature values of C_p for heptane¹⁶ (with the adequate correction for the difference of T_c between heptane and 2,4-dimethylpentane) and $\text{const} = 10$ one finds $B = 6400$ for $\text{LCST}/T_c = 0.87$ and $B = 2300$ for $\text{LCST}/T_c = 0.95$. One should note here that the thermodynamic functions and in particular C_p and its derivative in eq 15 have an analytical expression if a model for the liquid is used such as the van der Waals model (energy $= -1/v$).⁷ The experimental B has been well predicted⁸ for many nonpolar polymer-solvent systems. Since the quality of the prediction of the LCST from the theories varies from one polymer to another,^{7b,8,11} the exact values of T_∞ and B can stay as experimental parameters whose variation with solvent volatility is, however, well understood. On the other hand, near T_c , eq 15 is not expected to be a sufficient approximation. The linearity found for the standards in Figure 4 between $M_i^{-1/2}$ and the LCST up to the smallest MW of 4600 ($T_{1/2} = 192^\circ\text{C}$) is an assurance of the validity of the relation up to that MW.

The Constant T_∞ . This value can be obtained, as in the present work, with standards but also without them and with good confidence from the value of T_0 for a high MW sample as seen on Table I.

To resume, in an unknown polymer-solvent system, the evaluation of the constants does not represent a difficulty since they can be approximated as described above or obtained also by using in $W(\log M_i)$ the T_∞ and B values which fit best the MWD of a polydisperse polymer sample analyzed by another method.

Wesslau Distribution. The ln normal distribution function is expressed as³²

$$W(\ln M) = (\text{const})(\sigma^{-1}) \exp(-(\ln M - \ln M_{1/2})^2/\sigma^2) \quad (16)$$

Due to the analytical form of the above equation, the experimental data characterizing the distribution, $\sum h_{ii}^*$, become a linear function of $\ln M$ when plotted on a probability paper. Three characteristic values are marked on the line drawn through the experimental points, those

whose ordinates are, respectively, 0.5, 0.16, and 0.84. From the corresponding abscissa $M_{1/2}$, M_w , and M_n and the value of σ can be found by either of two relations: $\log \sigma = \log M_w - \log M_{1/2}$ or $\log M_{1/2} - \log M_n$. $M_{1/2}$ and σ , obtained as described above, have been used in eq 16 to calculate $W(\log M)$ for Marlex as plotted in Figure 6.

Turbidimetric Data for Marlex (Figure 1). For a solution ($\phi_2 = 0.02$) in 2,4-dimethylpentane and $v = 4$ K/min, a typical set of 20 peaks (T_i (°C); h_i (arbitrary units)) reads like this: 130, 0; 132, 2.8; 134, 4; 136, 7.5; 138, 7.8; 141, 15; 144, 20; 148, 26.5; 152, 22; 157, 27; 162, 22.5; 168, 23.8; 174, 19; 181, 16; 189, 15; 198, 8.5; 208, 7; 207, 7; 219, 8.5; 230, 1.5; 240, 0; $\sum h_i = 254.4$.

Registry No. HDPE, 9002-88-4.

References and Notes

- (1) (a) Billmeyer, F. W.; Stockmayer, W. H. *J. Polym. Sci.* **1950**, *5*, 121. (b) Schneider, N. S. *J. Polym. Sci., Part C* **1965**, *8*, 179. (c) Morey, D. R.; Tamblin, J. W. *J. Phys. Chem.* **1946**, *50*, 12.
- (2) Allen, G.; Baker, C. H. *Polymer* **1965**, *6*, 181.
- (3) Grubisic, Z.; Rempp, P.; Benoit, H. *J. Polym. Sci., Part B* **1967**, *5*, 753.
- (4) Urwin, J. R. "Molecular Weight Distribution by Turbidimetric Titration". In *Light Scattering from Polymer Solutions*; Hughlin, M. B., Ed.; Academic: London, 1972; p 789.
- (5) Delmas, G. *J. Appl. Polym. Sci.* **1968**, *12*, 839.
- (6) (a) Barbalata, A.; Delmas, G., submitted for publication. (b) Bohossian, T.; Delmas, G., submitted for publication. (c) Faucher, B.; Li, Xiao-dong; Delmas, G., submitted for publication.
- (7) (a) Prigogine, I.; Bellemans, A.; Mathot, V. *The Molecular Theory of Solutions*; North-Holland: Amsterdam, 1957; p 1. (b) Delmas, G.; Somcynski, T.; Patterson, D. *J. Polym. Sci.* **1962**, *57*, 79. (c) Patterson, T.; Delmas, G.; Somcynski, T. *Polymer* **1967**, *8*, 503. (d) Flory, P. J. *J. Am. Chem. Soc.* **1965**, *87*, 1833. (e) Orwoll, R. A.; Flory, P. J. *J. Am. Chem. Soc.* **1967**, *89*, 6822.
- (8) Delmas, G.; Patterson, D. *J. Polym. Sci., Part C* **1970**, *30*, 1.
- (9) Charlet, G.; Delmas, G. *Polymer* **1982**, *22*, 1181.
- (10) Charlet, G. Ph.D. Thesis, McGill University, Montreal, 1982.
- (11) (a) Kleintjens, L. A.; Koningsveld, R. *Colloid Polym. Sci.* **1980**, *258*, 711. (b) Koningsveld, R. *Adv. Colloid Interface Sci.* **1968**, *2*, 151. (c) Koningsveld, R. In *Characterization of Macromolecular Structure*; McIntire, D., Ed.; No. 573; National Academy of Sciences: Washington, D.C., 1968.
- (12) Société Nationale Elf Aquitaine, Lacq, France, Production 9,64170.
- (13) Lecacheux, D.; Lesec, J.; Quivoron, J. *J. Appl. Polym. Sci.* **1982**, *27*, 4867.
- (14) (a) Varennes, S.; Charlet, G.; Delmas, G. *J. Polym. Eng. Sci.* **1984**, *24*, 90. (b) Phi-Thi, T.-A.; Phuong-Nguyen, H.; Delmas, G. *Integration of Fundamental Polymer Science and Technology*; Kleintjens, L. A.; Lemstra, P. J., Eds.; Elsevier: London, 1986; p 77. (c) Besombes, M.; Menguel, J. F.; Delmas, G. *J. Polym. Sci.* **1988**.
- (15) Taylor, W. C.; Graham, J. P. *Polym. Lett.* **1964**, *2*, 169.
- (16) Rowlinson, J. S. *Liquid and Liquid Mixtures*, 2nd ed.; Butterworth: London, 1969.
- (17) (a) Beattie, W. H. *J. Polym. Sci.* **1965**, *3*, 527. (b) Meahan, E. J.; Beattie, W. H. *J. Anal. Chem.* **1961**, *33*, 632. (c) Beattie, W. H.; Jung, H. C. *J. Colloid Interface Sci.* **1968**, *27*, 581.
- (18) (a) Saeki, S.; Kuwahara, N.; Konno, S.; Kaneko, M. *Macromolecules* **1973**, *6*, 246, 589. (b) Cowie, J. M. G.; McEwen, I. *J. Polymer* **1975**, *16*, 224, 933.
- (19) Tompa, H. *Trans. Faraday Soc.* **1949**, No. 45, 1142. Bamford; Tompa, H. *Ibid.* **1950**, *46*, 310.
- (20) (a) Shultz, G. V. *J. Polym. Sci.* **1950**, *11*, 93. (b) Rayner, M. *G. Polymer* **1969**, *10*, 827.
- (21) Letot, L.; Lesec, J.; Quivoron, C. *J. Liq. Chromatogr.* **1980**, *3*, 427.
- (22) Kim, C. J.; Hamielec, A. E.; Benedek, A. *J. Liq. Chromatogr.* **1982**, *5*, 425, 1277.
- (23) Martin, M. *Chromatographia* **1982**, *15*, 426.
- (24) Hoffmann, M.; Urban, H. *Makromol. Chem.* **1977**, *178*, 2683.
- (25) Gunderson, J. J.; Giddings, J. C. *Macromolecules* **1986**, *19*, 2618.
- (26) Greschner, G. S. *Makromol. Chem.* **1982**, *183*, 2823.
- (27) Wild, T. R.; Ryle, D. C.; Knobloch, I. R.; Peat, J. *J. Polym. Sci., Polym. Phys. Ed.* **1982**, *20*, 441.
- (28) Glockner, G.; Van den Berg, J. H. M.; Meijerink, N. L. J.; Scholte, Th. G. In *Integration of Fundamental Polymer Science and Technology*; Kleintjens, Lemstra, Eds.; Elsevier: London, 1985; p 85.
- (29) Holzwarth, G.; Soni, L.; Schulz, D. N. *Macromolecules* **1986**, *19*, 422.
- (30) (a) Pope, J. W.; Chu, B. *Macromolecules* **1984**, *17*, 2633. (b) Chu, B.; Ondin, M.; Ford, J. R. *J. Phys. Chem.* **1984**, *88*, 6566.
- (31) (a) Galena, H.; Gordon, M.; Irvine, P.; Kleintjens, L. A. *Pure Appl. Chem.* **1982**, *54*, 365. (b) Galina, H.; Gordon, M.; Ready, B. W.; Kleintjens, L. A. *Polymers in Solution* Forsman, W. C., Ed.; Plenum: New York, 1986; p 267.
- (32) Zeman, L.; Biros, J.; Delmas, G.; Patterson, D. *J. Phys. Chem.* **1972**, *76*, 1206.
- (33) Peebles, L. H. *Molecular Weight Distribution in Polymers*; Wiley-Interscience: New York, 1971.
- (34) Randall, J. C.; Sieh, E. T. *NMR and Macromolecules*; Randall, J. C., Ed.; ACS Symposium Series 247; American Chemical Society: Washington, DC, 1984; p 131.